Topographic mapping of Mangawhai sand spit and development of a draft framework for monitoring future changes

Report prepared by Professor Mark Dickson, Associate Professor Murray Ford and Dr Emma Ryan, the University of Auckland, for Mangawhai Matters Inc and Mangawhai Harbour Restoration Society

Aug 2024

Date	Version	Description	Prepared by	Reviewed by
14-06-24	1.0	Draft 01	MD, ER, MF	Terry Hume
27-06-24	2.0	Draft 02	MD, ER, MF	Phil McDermott
09-08-24	3.0	Final report	MD, ER, MF	

THE UNIVERSITY OF AUCKLAND
NEW ZEALAND

Preface

The Mangawhai Harbour Restoration Society commissioned Auckland University to study the morphology of Mangawhai's barrier spit. The study, led by Professor Mark Dickson, mapped the landforms of the spit and developed a draft framework for monitoring future changes.

It was commissioned to help the Society understand the vulnerability to and consequences of the physical threats to the spit identified in the scoping study, *Mangawhai Harbour and Spit – Coastal Physical Processes and Management* (Hume Consulting Ltd for Mangawhai Matters Inc., July 2023). The threats include wind deflation, coastal erosion, and inundation by the sea.

Any increase in the intensity, duration, and frequency of storm events, along with increasing runoff from the catchment and sea level rise that might be associated with climate change will exacerbate and potentially compound these threats, even raising the possibility of a total breach creating a second, less sheltered entrance to the sea as occurred in 1978. Through detailed mapping of the spit's morphology, this study's findings provide the evidence needed to understand the possible impact of such events, identifying areas of particular vulnerability, gaps in our knowledge, and where monitoring need to be focussed.

This is one of a suite of studies that will also contribute to the Sustainable Mangawhai Project (www.mangawhaimatters.com). Others include studies of coastal inundation and catchment run-off. Jointly, they will enable the assessment of risks to the integrity of the harbour and distal spit, the consequences for the environment and community of any resulting damage, and the development of management plans to counter them. The results are intended to support decision making by the government and community agencies responsible for the future of the harbour on the basis that it reflects the best information and expertise available to assess and to respond to any threats.

This study provides up-to-date maps that illustrate in detail the form of the spit today. It goes further by providing links to computer-based versions of those maps, particularly useful for comparative purposes. Key changes taking place are revealed by comparison of the topographic data collected by drone surveys undertaken by the University of Auckland team in 2024 with airborne LiDAR surveys (2014 and 2018). The dynamics of the spit are clearly demonstrated in lateral erosion of the bay-side of the spit and the ocean-facing dunes. A considerable landward (westward) movement of the large dunes was recorded along with large net loss of sand over the spit between 2018 and 2014. Modelling of storm events and projected sea level rise indicates that relatively modest increases in sea level by 2040 are unlikely to materially change inundation and breaching risk associated with the typical annual storm. However extreme storms such as that in 1978 and increases in sea level by 2080 will allow even the annual storm to overwash and inundate low areas of the spit interior via low-lying and discontinuous parts of the dunes at the northern distal portion of the spit and at several locations on the ocean-side.

The report's findings are underpinned by comprehensive information on the techniques used. It provides a clear interpretation on what the risks are. Along with the priorities recommended for monitoring future changes to the spit, it provides a useful and important management tool.

Dr Terry Hume

9 August 2024

CONTENTS

EXECUTIVE SUMMARY

A survey of the topography of Mangawhai Spit was conducted in 2024 using a drone-based LiDAR system, which allowed for a comparison of topographic changes with data from an earlier aircraft-based LiDAR survey conducted in 2018. A web-platform is provided to visualize digital elevation models (DEMs) as well as historic photographs and digitised coastlines, which provide an overview of historic changes to Mangawhai Spit.

Water levels were calculated for extreme events, including the future effects of sea level rise (SLR). This enabled maps to be drawn identifying potential points for breakthroughs by the sea and flow paths through which water might penetrate the spit leading to potential flooding from the sea. The information provides baseline data against which to monitor future change. The report concludes with guidance and options for monitoring future change.

Key findings:

- The topography of the low-lying interior of the spit has not appreciably changed between 2018 and 2024.
- Lateral erosion of the bay-side spit has occurred while the ocean-facing dunes in the northern part of the spit have increased in elevation.
- Considerable (10-25 m) landward (westward) movement of the large dunes in the southern part of the spit has occurred between 2018 and 2024; it is not clear whether this is part of a longer-term westward movement of the dunes, but it is notable that decadal-scale landward erosion of the ocean-facing dunes has occurred at average rate of about 1.4 m/y and that other paleo-environmental research suggests east-to-west movement of dunes over centuries.
- Net loss of sand over the spit between 2018 and 2014 is ~260,000 m^3, which is equivalent to 26,000 standard dump trucks (~10 cubic metres per load) or about 8 cm over the entire spit, representing about 1.8% of the total spit sand volume.
- Bathtub modelling indicates that a typical annual storm coinciding with spring high tide is unlikely to inundate the spit, but there are at least two areas toward the southern end of the spit that have local low points in the dunes that could potentially overtop.
- Relatively modest increases in sea level by 2040 are unlikely to materially change inundation and breaching risk associated with the typical annual storm.
- By 2080, if the morphology of the spit does not naturally adjust upward in response to SLR, the annual storm is likely to inundate the spit both through the distal northern portion of the spit and at several discrete locations on the ocean-side of the spit where the dunes are low-lying and discontinuous.
- A storm with similar properties to the 1978 storm would likely produce total water levels of around 3.2 m that would inundate large portions of the barrier with overwashing in several ocean-side locations that could potentially stimulate breaching; however, today the spit is notably wider than it was in 1978 meaning that the spit is less vulnerable to breaching today than it was in 1978.
- Extreme dynamic total water levels of 4.7 m (with runup) have been modelled for the open coast of Mangawhai by Tonkin and Taylor (2021, Table 2.5 and Appendix C) based on a 1% Annual Recurrence Interval. Such an extreme storm would overtop the dunes in many places and create conditions under which breaching is likely.
- The bathtub models provided in this report rely on an assumption that a constant elevated water surface remains for the length of time required to achieve that

level of inundation. However, storms may not elevate the water level for a sufficient time to inundate the spit in the way bathtub models suggest. Detailed dynamic modelling is required to investigate these effects, which was beyond the scope of this study.

- Using slope maps and simple hydraulic modelling we estimate likely flow paths across the spit. The distal northern area of the spit contains a local low point that can be inundated by elevated water levels. Several possible overwash/inundation locations on the open coast of the spit are also identified, one of which nearly connects through to a flow path on the bay side of the spit.
- We draw attention to historic movements of the estuary channel leading up to breaching in 1978. It appears that potential bay-side breach initiation is likely to be controlled by the position of the harbour channel. The spit neck was unusually narrow prior to breaching in 1978 and the harbour shoal adjacent to the spit neck was unusually wide. Between 1963 and 1978 the channel flow appeared to be focused on the narrow portion of the spit neck leading to its progressive narrowing. The direction of flow appears to have been influenced by the widening of the adjacent shoal. The narrow width of the spit neck made the spit particularly vulnerable to breaching during the extreme 1978 storm.
- We recommend monitoring of Mangawhai spit, with particular focus on the position of the estuary channel, the growth of the estuary shoal adjacent to the spit neck, the width of the spit neck, and ongoing east-to-west movement of the beach shoreline and spit dunes.

LIST OF ABBREVIATIONS

AMSL	Above Mean Sea Level
ARI	Annual Return Interval
AT	Astronomical Tide
DEM	Digital Elevation Model
GCMs	Global Climate Models
GCPs	Ground Control Points
GIS	Geographic Information System
Hs	Significant wave height
LAT	Lowest Astronomical Tide
LiDAR	Light Detecting and Ranging
LINZ	Land Information New Zealand
MHRS	Mangawhai Harbour Restoration Society
MHWS	Mean High Water Spring tide
MSL	Mean Sea Level
NZVD2016	New Zealand Vertical Datum 2016
<n>	Wave setup
R	Runup
SfM	Structure from Motion
SLR	Sea Level Rise
SS	storm surge
TWL	Total Water Level
TWLr	Total Water Level including wave runup

LIST OF FIGURES

1. Theoretical framing for understanding Mangawhai spit and potential breaching

Mangawhai sand spit is an example of a 'barrier': a long, narrow deposition of sand parallel to the coast that is not submerged by the tide (Kraus et al., 2008). Barriers protect the land and water behind them, particularly during storms, by reducing storm surge and wave energy (Hoagland et al., 2023).

Overwash and breaching are storm-induced impacts on barriers that are a natural part of barrier evolution but can have adverse impacts on ecosystems and local communities (Plomaritis et al., 2018; Stretch & Parkinson, 2018). Overwash occurs when water and suspended sediment travel across the barrier, limited by frictional effects (Donnelly et al., 2006). Breaching occurs when a channel forms connecting the seaward and landward sides of the barrier (Kraus et al., 2002; Donnelly et al., 2006).

Breaching is often associated with overwash. Several morphological factors influence vulnerability to overwash and breaching, including dune height, barrier width, barrier volume, and back-beach elevation (Plomaritis et al., 2018; Donnelly et al., 2006). Important storm characteristics include storm surge, storm frequency, orientation of the coast relative to the storm, onshore winds, spring high tides, and storm waves (Fletcher et al., 1995).

A lot of emphasis has been placed on ocean-side barrier processes, including wave runup and dune height interactions (e.g. Sallenger, 2000; Stockdon et al., 2009; Hoagland et al., 2023). Sallenger (2000) identified four regimes: (1) 'swash' where runup is confined to the foreshore; (2) 'collision' where runup begins eroding dunes, (3) 'overwash' when runup exceeds the dune crest or local low points within hummocky dunes; (4) 'inundation' where the barrier is submerged, likely forcing a new inlet. However, breaching could also occur in other phases, not just inundation.

Ocean-side processes are important, but breaching often involves both ocean and bay-side processes, with water elevation differences on either side of the barrier influencing the direction of flow and breaching potential (Kraus et al., 2008; Over et al., 2021). Some evidence from international case studies indicates that breaching may be mainly caused by bay-side processes, and that bay-side surge can be higher than ocean-side surge (Over et al., 2021). After storms make landfall there can be elevated water levels on the bay-side of barriers, leading to a land-to-sea outwash regime that triggers breaching from the bay-side (see Over et al., 2021). Storm duration is important because it influences the water level lag time between the bay and ocean sides of the barrier (Basco & Shin, 1999).

Storm duration and bay-side elevated water levels may be a key risk factor at Mangawhai, but these processes are not well understood. The international literature emphasises the complexity of overwash and breaching processes and the need for integrated approaches in storm impact assessment and barrier management. Breaching can be initiated either on the ocean-side or bay-side as a result of elevated water levels. It might take the form of outwash (bay-side) or overwash (ocean-side) channel scour, or through liquefication of sands, or a combination of both.

2. 2018 LiDAR

Figure 1 and Figure 2 respectively show a 1m resolution DEM and DEM Hillshade model created from the Northland Regional Council airborne LiDAR (2018-2020) obtained through the LINZ data service. The models have a horizontal resolution of 1 m and vertical accuracy of ~0.2 m.

The DEMs very effectively capture the large-scale features of Mangawhai Spit, including the large sand dunes of >40m elevation (AMSL, above MSL) on the southern region of the spit and the depression in the central region.

The toe of the foredune on the seaward side of the spit occurs at approximately 2 m AMSL (above Mean Sea Level) and an area of relatively low and narrow foredunes is apparent in the central region of the spit adjacent to the low depression landward of these dunes. This is close to the area that was breached in 1978.

3. 2024 drone-LiDAR

We undertook a drone-based LiDAR survey of Mangawhai sand spit on 9 April 2024. The survey was conducted by Recon Ltd using two LiDAR systems (L1 and L2) running concurrently. This made it possible to capture the spit morphology within about 2 hours of low tide, which allowed maximum coverage of the spit close to the spring low tide level (1330 Low tide, ~0.13 m above LAT). 20 Ground Control Points (GCPs) were accurately positioned by the University of Auckland using Real-time Kinematic GPS. These GCPs were used to constrain the LiDAR data. The vertical error for models created from the LiDAR data is ~0.046 m (RMSE) with about 200 points per meter captured. Hence, the drone-based LiDAR was approximately 4 times higher resolution in vertical accuracy.

To directly compare the 2018 and 2024 LiDAR we down-sampled the 2024 LiDAR to a 1m DEM. Figure 3 shows a 1m DEM from the 2024 LiDAR and Figure 4 shows a Hillshade model from the 2024 LiDAR.

The datum for all surveys was NZVD 2016.

4. DEM of difference

Down-scaling the 2024 drone-LiDAR to 1m enables direct comparison of physical change in Mangawhai Spit between 2018 and 2024. Figure 5 shows a DEM-of-difference with blue colours showing areas where the spit has increased in elevation and red showing areas where elevation has decreased. Areas of negligible change are shown as white. GIS tools such as 'hillshade', 'surface difference', 'slope', 'volume change', and 'cut and fill' were used to calculate surfaces.

The low-lying interior of the spit has not appreciably changed between 2018 and 2024. The ocean-facing dunes in the northern part of the spit have increased in elevation. Lateral erosion of the bay-side spit has occurred, with erosion of up to 15m in places. Erosion of this bay-side coast should be monitored, because over time this can reduce the width of the spit making it more vulnerable to breaching. Landward (westward) movement of the large dunes in the southern part of the spit is particularly notable. The apex of the dune appears to have moved about 10-25 m to the west in different parts of the dune. It is not clear whether the landward movement is specific to the observation period (2018-2024) or part of a longer-term trend. More data are required to clarify this, but it is worth noting the paleo-

environmental study conducted by Enright and Anderson (1988) on Mangawhai spit, where they argued that over a period of hundreds of years, 'Net east to west movement of sands has resulted in a large deflation surface near the coast'. The DEM-of-difference between 2018 and 2024 shows net east to west movement of the dunes that is consistent with the longer-term pattern referred to by Enright and Anderson (1988). However, we have only two data points in 2018 and 2024 and to corroborate whether this trend is chronic requires more data.

Figure 6 shows a cut-and-fill analysis to evaluate the net gain and loss of sand on the spit between 2018 and 2014. The net loss is ~264,700 m^3 of sand, equivalent to ~26,000 standard dump trucks (~10 cubic metres per load). Another way to visualize this is to imagine equal loss of sand across the spit. The spit area is ~3,166,942 m^2, meaning about 0.08 m^3 of sand lost per square meter, which is roughly equivalent to removing a layer of sand ~8 cm deep from each square meter of the entire spit. The spit volume (relative to NZVD 2016) in 2024 was ~14,477,658 m^3, meaning that the material lost between 2018 and 2024 was about 1.8% of the total volume of sand. This strikes us as quite a large number. We also direct readers to recently published national coastal change data (Appendix 8.1) which show that dune toe at Mangawhai spit appears to have eroded at an average rate of about 1.4 m/y over the past ~59 years, which is considerable. Note that this rate applies mainly to the southern part of the spit due to mapping uncertainties in the northern area. Historic aerial photographs show that the southern part of the spit has shunted east-to-west by about 100m in places, which is significant.

It is difficult to offer definitive statements in relation to the implications of the westward movement of the barrier spit, including its large dunes. We are unclear whether the movement of the westward movement of the spit is transitory or part of a longer-term pattern. More monitoring data are required, but the net east to west movement that we have mapped with drone data are consistent with the net east to west movement seen in the historical photographs, and also the net east to west movement described over centennial time scales by Enright and Anderson (1988). Further monitoring is warranted. One consideration is that Cyclone Gabrielle has somewhat inflated the recent beach and dune-toe erosion data. Before and after satellite images from the east coast of the North Island show that erosion of 5-10 m of the dune along the east coast of Northland was typical, with some "hotspots" of erosion up to 15m.

5. Structure-from-motion survey

We subcontracted a commercial provider to capture the drone-LiDAR described in section 3. The total cost was $9,890 inc GST. This did not include the cost of establishing survey control, which was undertaken by the University of Auckland, nor the cost of transport around the spit that was covered by MHRS. Hence, ongoing monitoring with a commercial drone-LiDAR operator would not be less than $10,000 per survey.

On the same day as the drone-LiDAR survey (9 April 2024) we tested another viable method of obtaining a high-resolution DEM from drone-based photographs on a small section of the spit. Structure-from-Motion (SfM) is a photogrammetric technique that reconstructs 3D morphology from a collection of overlapping 2D photographs. The approach uses common features and patterns across multiple images, estimating 3D positions of these features, and recursively adjusting parameters to minimise reprojection errors. Processing times are quite long, but usually it is possible to build dense point clouds and high resolution DEMs with this approach. Initially I was concerned that the spit would not have enough pattern for this method, but actually the technique worked very well. The easiest way to visualize the outputs of the

LiDAR and SfM models is by comparing them side-by-side. We have made the outputs available on a webview using the links below, and Figure 7 provides a snapshot comparison.

https://murrayford.users.earthengine.app/view/mangawhai-aerial-viewer

The SfM model has a resolution of ~0.04 m, which is comparable to the 2024 LiDAR resolution. Hence, it is apparent that SfM does provide a viable alternative to LiDAR. A rough estimate is that UoA could probably provide a full SfM survey of the spit at about 25-50% less than the cost of a drone-LiDAR survey.

The webviewer also makes it clear that the photography enabled both from SfM and LiDAR survey can be very useful for a range of purposes, including mapping areas of vegetation and shell and areas of cultural significance.

6. Slope map and water path prediction

The maps produced in section 6 rely on an assumption that a constant elevated water surface remains for the length of time required to achieve that level of inundation. In reality, storms move, winds abate, and wave heights return to normal levels. Many storms may not elevate the water level for a sufficient time to inundate the spit in the way suggested by the maps in section 6. A detailed dynamic model would be required to investigate these effects, which was beyond the scope of this study.

Figure 8 provides a simple method to get a sense for the likely flow path based on local slope across the spit. In the distal northern area of the spit there is a local low point that can be inundated by elevated water levels, with flows travelling to and accumulating in the central low region. The slope and flow model also draws attention to several possible overwash/inundation locations on the open-coast of the spit, and one of these nearly connects through to a flow path on the bay side of the spit.

Figure 9 provides a way to visualise slope and aspect draped on a hillshade model. The advantage of this figure is that it helps to visualise local low points that might be vulnerable to breaching. These areas have been identified by studying the bathtub maps (e.g. Figure 12), slope and flow path map (Figure 8) and the aspect and slope map (Figure 9). Note that potential bay-side breach initiation is likely to be controlled by the position of the harbour channel (section 8) and we have not identified likely bay-side breach locations.

Historic breaching at Mangawhai has been reasonably well documented (e.g. McCabe et al., 1985) and we have not attempted to reassess any of that work in this report. However, we have produced a web viewer (see section 8.1) that provides an excellent visual summary of the events leading up to the breach. It is apparent that the spit neck was unusually narrow in 1963 and that the harbour shoal adjacent to the spit neck was unusually wide. The effect was that the channel flow appeared to be focused on the narrow portion of the spit neck. The spit neck continued to narrow to 1978 and the shoal continued to widen. The narrow width of the spit neck made the spit particularly vulnerable to breaching during the extreme 1978 storm.

Unfortunately, no elevation data are available from 1978, which means it is not possible to determine whether the split was 'deflated' in 1978 relative to its current elevation. It seems likely that in 1978, flooding of the narrow spit from the bay (harbour) side was an important process leading to breaching, and that a similar process in the future could be a threat. Figure 8 shows that water can most easily

inundate the spit from the northern distal region of the spit, but our judgement is that breaching of the spit is most likely in the narrowest part of the spit where it has breached before (i.e. point 4 on Figure 9). We speculate that spit narrowing over time is influenced by the relationship between the harbour shoal and channel position. Growth of the shoal has potential to direct flows into the narrow portion of the spit, leading to further narrowing. During a severe storm, similar to the 1978 storm, then super elevated water levels could lead to inundation from bay-side (and possibly the northern part of the spit), and if waves were able to breach the central narrow point identified on Figure 9, then there would be a relatively narrow point that could connect the ocean with the channel.

7. Total Water Level (TWL) calculation and bathtub modelling

A common approach to estimating the future impacts of SLR or coastal flooding is to implement a passive 'bathtub' model. This simple approach involves projecting the water level in question onto a DEM. We projected our TWL calculations onto the 2024 LiDAR to achieve this effect. We estimated TLW and TWLr (including wave runup) using the following approach:

TWL = AT + SS + SLR + <n>

And

TWLr = AT + SS + SLR + R

Where AT = Astronomical Tide, SS = storm surge, R = runup, <n> = wave setup and SLR = sea level rise.

Analyses were conducted in R Studio. Astronomical tide data were sourced from the NIWA tide forecaster for the periods 31/12/2022 – 31/12/2023 (present) and 31/12/2029 – 31/12/2030 (for all future scenarios). Tide data were converted to NZVD2016 using the elevation of mean sea level relative to NZVD2016 at the closest primary tide gauge at Marsden Point. Average mean sea level elevation of -0.16 m (NZVD 2016) was obtained for the period 1995 – 2014 (MfE, 2024). The highest 5% of spring tides were averaged to provide a mean high water spring tide (MHWS) value for Mangawhai of 0.92 m above MSL for the present day, and 0.95 m for future scenarios.

Storm surge is the measure of the elevation of the sea above the predicted astronomical tide due to: 1) the barometric set-up from low atmospheric pressure, and 2) wind stress. Modelled storm surge data were sourced from https://coastalhub.science/storm-surge based on the work of Cagigal et al 2020 for the model period 1/1/2015 – 31/12/2085. The model data include estimates of storm surge under a range of global climate models (GCMs). We used four scenarios from two of the best performing GCMs (ACCESS1.0-RCP4.5, ACCESS1.0-RCP8.5, MIROC5-RCP4.5 and MIROC5-RCP8.5). The Cagigal et al. (2020) dataset presents relatively low storm surge values, averaging 0.14 m for Mangawhai open coast. This may be because the models are trained using GCM data from a relatively short period (1992 – 2014) during which there were no east coast storms that approached the intensity of the 1978 storm at Mangawhai.

SLR data were sourced from NZSeaRise (https://searise.takiwa.co/map/) and downloaded for the time period 2005 – 2150 under SSP2-4.5 and SSP5-8.5. For future TWL scenarios, SLR data were averaged over a ten-year period around 2040 (i.e. 2035 – 2045) and 2080 (i.e. 2075 – 2085).

Wave runup is a function of wave setup (<n>) and swash (S), and was estimated using the following approach after Stockdon et al. (2006) and Dalinghaus et al. (2023):

$$R = \langle n \rangle + S/2$$

$$\langle n \rangle = 0.355 H_{so} \xi_o^{0.5}$$

$$S = \sqrt{[(0.06(H_{so} \times L_o)^{0.5})^2 + (0.75 B_f \times (H_{so} \times L_o)^{0.5})^2]}$$

Where H_{so} = significant wave height of offshore waves
ξ_o = Iribarren number of offshore waves ($\xi_o = \tan\alpha/(H_{so}/L_o)^{0.5}$)
L_o = wave length of offshore waves ($gT^2/2\pi$), where T is wave period
B_f = slope of the foreshore

An average foreshore slope of 0.0425 was used based on data obtained from Northland Regional Council. Modelled wave data (Hso, T and Lo) were sourced from Albuquerque et al. (2021, 2022) (https://coastalhub.science/data). The wave hindcast and projections use a range of GCMs and for this study we used four scenarios from two GCMs (ACCESS1.0-RCP4.5, ACCESS1.0-RCP8.5, MIROC5-RCP4.5 and MIROC5-RCP8.5).

To generate TWL and TWLr we averaged the top 1% of significant wave height. These waves are representative of a typical annual storm, and when coincident with spring high tides, we estimate these conditions would occur on average 1.3 times per year. We conducted bath-tub style modelling using TWL and TWLr from different SLR scenarios superimposed on the 2024 drone-LiDAR DEM (Table 1). For visualization, we present the average TWL across the four GCMs for the SSP8.5 p83 SLR scenario only (the highest sea level increase modelled in this study).

Table 1: Total water level excluding (TWL) and including (TWLr) wave runup, in m relative to NZVD2016 for Mangawhai sandspit open coast in the years 2020, 2040, 2080. Values used in maps are provided in bold.

		TWL (m) AND YEAR			TWLr (m) AND YEAR		
MODEL	SLR scenario	2020	2040	2080	2020	2040	2080
ACCESS 4.5	SSP2 4.5 - p17	1.512	1.626	1.827	2.489	2.403	2.634
ACCESS 8.5		1.513	1.610	1.829	2.49	2.377	2.606
MIROC 4.5		1.512	1.613	1.843	2.489	2.54	2.9
MIROC 8.5		1.509	1.620	1.834	2.486	2.547	2.751
ACCESS 4.5	SSP2 4.5 - p50	1.542	1.676	1.937	2.519	2.453	2.744
ACCESS 8.5		1.543	1.660	1.939	2.52	2.427	2.716
MIROC 4.5		1.542	1.663	1.953	2.519	2.59	3.01
MIROC 8.5		1.539	1.670	1.944	2.516	2.597	2.861
ACCESS 4.5	SSP2 4.5 - p83	1.572	1.706	2.087	2.549	2.513	2.894
ACCESS 8.5		1.573	1.690	2.089	2.55	2.487	2.866
MIROC 4.5		1.572	1.693	2.103	2.549	2.65	3.16
MIROC 8.5		1.569	1.700	2.094	2.546	2.657	3.011
ACCESS 4.5	SSP5 8.5 - p17	1.512	1.706	1.947	2.489	2.433	2.754
ACCESS 8.5		1.513	1.690	1.949	2.49	2.407	2.726
MIROC 4.5		1.512	1.693	1.963	2.489	2.57	3.02
MIROC 8.5		1.509	1.700	1.954	2.486	2.577	2.871
ACCESS 4.5	SSP5 8.5 - p50	1.542	1.706	2.067	2.519	2.473	2.874
ACCESS 8.5		1.543	1.690	2.069	2.52	2.447	2.846
MIROC 4.5		1.542	1.693	2.083	2.519	2.61	3.14
MIROC 8.5		1.539	1.700	2.074	2.516	2.617	2.991

ACCESS 4.5	SSP5 8.5 - p83	1.582	1.706	2.247	2.559	2.523	3.054
ACCESS 8.5		1.583	1.690	2.249	2.56	2.497	3.026
MIROC 4.5		1.582	1.693	2.263	2.559	2.66	3.32
MIROC 8.5		1.579	1.700	2.254	2.556	2.667	3.171
ENSEMBLE AVERAGE FOR SSP5 8.5 – p83		**1.58**	**1.71**	**2.25**	**2.56**	**2.59**	**3.14**
1978 OBSERVED (MCCABE ET AL 1985)		**-**	**-**	**-**	**3.2**	-	-
1% ARI (TONKIN AND TAYLOR, 2021)		**-**	**-**	**-**	**4.7**	-	**5.7**

GIS tools were used to project TWL onto the 2024 DEM. The approach involves specifying a water level elevation that spreads and finds areas at or below that elevation. If it reaches a cell with an elevation that is higher, it marks the cell as impassable and the cells behind the barrier are marked as not flooded. The inundation model ends once the spread of the "flood" cells cannot spread any further. Inundation surfaces were created using a 0.5 m resolution raster based on the 2024 LiDAR to enable enhanced detail in the model. Flowlines were created using 'Fill' 'Flow Direction and Accumulation' tools.

Figure 10 shows bathtub inundation for 2024 based on TWL of 1.58m (approximately the annual storm) and TWLr of 2.56 m, which includes runup. Note that we clip the TWLr overlay so that only the seaward side of the spit is exposed to wave runup. We consider it unrealistic to represent runup on the bay-side of the spit (although some bathtub models do include runup without this consideration).

There are two advantages in the way we present Figure 10. First, we can conclude based on a typical annual storm coinciding with spring high tide, that the interior of the spit is unlikely to be inundated. Second, we observe that with wave runup, there at least two areas toward the southern end of the spit that are likely to see wave overtopping and that these areas represent potential vulnerabilities to breaching. Figure 11 shows only marginal change from Figure 10, indicating that the relatively modest increase in sea level by 2040 is unlikely to materially change inundation and breaching risk associated with the typical annual storm. In contrast, by 2080 (Figure 12), if the morphology of the spit does not naturally adjust to SLR, the annual storm (TWL) is likely to inundate the spit, both through the distal portion of the spit where the dunes are low-lying and discontinuous, and as a result of runup (TWLr) overtopping the dunes in several low points on the ocean side of the barrier.

If the barrier does not naturally adjust its morphology to SLR, the risk of breaching due to the annual typical storm is likely to be very high in 2080 because of the effects of SLR. Note that sandy beaches and barrier spits are expected to naturally adjust to SLR. Cooper et al., (2020) explain that sandy beaches are highly varied in form and that it is widely accepted that there is no single response to SLR. Some beaches migrate landwards under SLR due to onshore sediment transport without loss of beach width. In this case, dune height might keep pace with SLR. However, dunes might also degrade due to erosion under SLR and offshore sediment transport can occur also. Mangawhai spit will respond to SLR adjusting its morphology, but it is unclear exactly what the nature of the response will be. The historical east to west movement of the spit is relevant in this context and should be monitored.

In addition to the future effects of SLR, Mangawhai spit is exposed currently to extreme storm conditions. We have run two models to simulate extreme scenarios. First, we map a TWLr value of 3.2 m (Figure 13) to simulate a storm with similar properties to the 1978 storm (McCabe et al., 1985). Second, we present a map of TWLr generated from extreme dynamic water levels modelled by Tonkin and Taylor (2021) (Figure 14), which considers an extreme 1% Annual Return Interval (ARI)

(i.e. a 1% chance in any single year) significant wave height of 8.6 m (Tonkin and Taylor, 2010 Table 2.5), which is up to 3 m higher than the wave data we have used to calculate TWL and TWLr in other scenarios.

Figure 13 indicates that the 1978 storm today would inundate large portions of the barrier and that overwashing in several ocean-side locations is likely, and these could potentially stimulate breaching. Today the spit is notably wider than it was in 1978 (see section 8), and we are unsure on the extent to which this additional width would reduce the chance of breaching.

Figure 14 (8.6 m offshore Hs) presents a significantly more extreme scenario than presented in Figure 13 (the 1978 storm). We have not attempted to verify whether the Tonkin and Taylor (2021, Appendix C) dynamic water level value of 4.7 m is reasonable for the Mangawhai open coast. Note that this value includes wave runup, so we have not projected it to the estuary side of Mangawhai. This value implies that were this extreme storm to occur today, there would be a lot of overtopping throughout the barrier, raising the prospect that catastrophic breaching could occur. We recommend further research to clarify the expected total water levels at Mangawhai under these extreme conditions.

8. Appendices

8.1 A web-platform to visualize DEMs, historic photographs, freely available satellite images, and historic coastal change mapping

We have developed three web viewers:

1) Public viewing of historic vertical aerial photographs captured in 1963, 1978, 1983, and 1995 (Figure 15):
   https://murrayford.users.earthengine.app/view/mangawhai-aerial-viewer

2) Mapped coastline positions through time (Figure 16):
   https://murrayford.users.earthengine.app/view/mangawhaiaerialsandlines

3) Example freely available satellite images (Figure 17):
   https://murrayford.users.earthengine.app/view/mangawhais2viewer

We also direct readers to coastalchange.nz where our recent nation-wide coastal change mapping was published on 02/08/24. The mapping indicates considerable historic erosion of the ocean-side of Mangawhai spit at a long-term average rate of ~1.4 m per year over the last 59 years.

8.2 Suggestions for monitoring

Historical photographs make it clear that Mangawhai spit was particularly prone to breaching during 1978. The neck had progressively narrowed between 1963 and 1978, likely as a result of the growth of the shoal in the harbour immediately adjacent to the neck of the spit. The shoal appeared to direct flow into the spit neck, further reducing its width. The historically large storm of 1978 was then able to breach the spit as a combined result of elevated water levels both on the ocean-side and bay-side of the spit. The scientific literature states that breaching can be initiated either on the ocean-side or bay-side of sand spits. Monitoring of Mangawhai spit should include both sides of the spit and the eastern flank of the shoal.

Satellite monitoring

Satellite monitoring should form a component of a future monitoring plan. There are a variety of ways to monitor the spit using optical satellite imagery, which provides visual true colour images, along with additional information from non-visible light, which can be used to separate water from land automatically and to measure vegetation health. Optical images can be accessed from commercial providers or providers of free government imagery.

Commercial satellite imagery

Commercial providers sell satellite imagery at resolutions ranging from ~0.30 m through to ~5 m. Users can access archival imagery which is imagery that has already been captured, or task satellites to collect new images. Each approach provides different opportunities and levels of complexity and cost with respect to coastal monitoring.

Archival imagery is cheaper than tasking and has the benefit of allowing a user to inspect imagery before purchasing. However, this approach assumes there will be suitable imagery available during the period of interest. Given the growing number of commercial providers, usually there are <1 m resolution images available within time periods of 3-6 months. Coarser resolution (3-4 m) images are available at near-daily sampling intervals.

Two challenges limit the use of commercial satellite imagery for monitoring at Mangawhai:

1) Orders of archival imagery of Mangawhai spit are likely to be small and sales teams generally show little interest in low-volume orders. Companies are emerging that provide access to imagery via websites that are relatively simple to use, similar to any online shopping platform. The most well-known platform is SkyFi (www.skyfi.com), but this and similar providers don't yet sell imagery from many of the larger satellite operators, so there is usually less imagery available for any given location.

2) Imagery is often expensive, with typical costs for the highest quality imagery (i.e. 30 cm resolution) at ~$30 per km^2, with different providers having a complex array of minimum order sizes (some at 25km^2) and other factors that impact price. Coarser resolution imagery can be very affordable via SkyFi, with 3 m imagery currently available for $2.50 (USD) per km^2, with minimum orders of only 5 km^2. So there is a lot of variability in relation to image acquisition, but to obtain images for Mangawhai, the costs should generally be less than <$USD100 per image.

If an image is required on a specific date or within a window of time (e.g. to monitor a storm), it is possible to "task" a satellite, in which a user requests for a satellite to capture a designated area. A number of variables impact tasking price including resolution, minimum cloud cover and the time period of the imagery required. A coarser resolution imagery, with <50% cloud cover, collected at some point during a 2-week interval is cheaper than a 30 cm resolution image collected ASAP. There is some risk associated with tasking, for example, an image might meet your criteria (i.e. <20% cloud) but still have cloud over an important area of interest.

SkyFi.com is the most intuitive and easy platform for consumers to task satellite imagery. Below is indicative pricing for 25 km2 of imagery at different resolutions from SkyFi.com. The collection windows is between 3-4 weeks, however, for an additional price the orders can be prioritized for a 2-3x increase in price.

- 15-30cm ($750 USD)
- 30-50cm ($300 USD)
- 50-100cm ($200 USD)

Free Government imagery

The US government and European Union operate optical satellites that provide free access to imagery. The US programme is called Landsat and collects imagery every 8 days at 30 m resolution. The European programme, known as Sentinel 2, collects imagery every 5 days at 10 m resolution.

Both Landsat and Sentinel 2 imagery are widely used for monitoring shoreline change using the position of the waterline as the shoreline proxy (i.e. Vos et al., 2019). This approach has become very popular in recent years as the imagery used is free to access and the algorithms used to detect the waterline can be run at large scales. In general, the coarse resolution of the Landsat and Sentinel 2 imagery is most useful for generating high frequency time series of positions (i.e. every 5-8 days) of shoreline position with relatively large positional uncertainty (>10 m).

Figure 17 provides an example of the resolution of different satellite imagery products. A dynamic example can be found at:
https://murrayford.users.earthengine.app/view/mangawhais2viewer

This application shows an example of the average Sentinel 2 image for each year from 2017-2023 alongside the latest Sentinel 2 image with less than 25% cloud cover. Landsat and Sentinel 2 imagery provide a useful snapshot of the barrier and could be useful for identifying large scale changes help identify areas to prioritise for more detailed commercial satellite or drone-based monitoring. The application will update every time a new Sentinel 2 image is collected that has <25% cloud cover. The free application that we have built could be used for sub-annual monitoring of the channel position, harbour shoal dimensions and Mangawhai spit neck width.

LiDAR monitoring

DEM monitoring should be conducted at the temporal resolution made possible by airborne LiDAR, perhaps every several years. Typically LiDAR surveys are flown at low tide, and this would be important to capture the tidal shoal. Two surveys are now available (2018 and 2024). These surveys show that the dunes have been moving landward and that the barrier has lost sand between 2018 and 2024. When the next LiDAR survey is flown by Northland Regional Council we suggest that a third DEM be created and subtracted from the 2018 and 2024 DEMs to identify whether there is any further sand loss, with subsequent investigation into whether this constitutes a trend. Costs associated with contracting someone to produce a new DEM and comparing it with older DEMs and analyse the results are relatively modest (e.g. ~$2,000). If there is need and interest, targeted LiDAR could be flown by drone (cost of the survey in this report ~$10,000), but costs might be less (25-50% less) if SfM is used rather than drone-LiDAR.

Targeted monitoring

Targeted inspection and monitoring could be conducted of the sites we have identified in this report as low points that are potentially vulnerable to inundation. It would be useful to monitor these sites during an extreme event to ground-truth the manner in which elevated water levels could potentially affect them. The inundation maps we provided in section 6 are subject to uncertainty, because they assume water levels remain elevated for a duration that can inundate the spit. Ground-truthing during a storm would provide further insight in this regard.

Ground-truthing an event would be time-consuming. A student project would be ideal, but waiting for storms is not ideal for a student project. Monitoring a storm at commercial rates and analysing the results would likely cost $5,000 - 15,000, depending on experiment design.

Calculations to identify sand volumes to fill gaps in dunes

In Figure 9 we identified within the detailed DEM from the drone-LiDAR several potential low points within the dunes. It would be useful to undertake calculations of the size of the dimensions of these low spot gaps to estimate how much sand would be required to plug the gaps against storm events, or potentially build up the size of the existing dunes up and down coast. Fieldwork would be required to ground-truth the gaps and work through logistics.

Summary table of monitoring options

Cost	**Method**	**Capability required**
Low	Regular (i.e. 1-6 monthly) monitoring of the barrier using freely available satellite imagery (i.e. Landsat/Sentinel 2). Monitoring should focus on a) movement of the channel and shoal within the estuary, and b) barrier thinning. Shoal migration and barrier thinning are likely leading indicators of future breaching and could be tracked across different timescales depending on the pace of change. Regular community-lead observations (perhaps including repeated photographs from the same location) of areas identified as being vulnerable to inundation (selected points on Figure 9). Observations around the current erosional state of vulnerable areas identified in the inundation modelling to capture any evidence of erosion (i.e. erosional scarps) or wave runup levels (i.e. debris lines) following spring tides or large wave events.	Moderate level of capability required. Open-source tools exist that would require some upskilling to implement. There are options that are suitable to intermediate-level user (i.e. integrating imagery into Google Earth to make measurements of shoal position). Maintaining a record of community observations requires basic data handling capabilities and careful repetition of photograph locations. This could potentially be achieved by inserting a stake and camera mount at selected photograph locations.
Moderate	Develop and implement annual monitoring of the shoal and location of historic breach using high resolution satellite imagery (i.e. 50cm resolution). Satellite imagery costs vary considerable depending on provider, ~$300-500 per image. Monitoring	Moderate to high level of capability required to purchase, process and analyse commercial satellite imagery. Computer-competent user could be trained in the methods, or it could relatively easily be outsourced to a consultant

	could map the toe of the dune along areas of previous breaching and in areas identified from inundation modelling. Analysis of council/central govt. captured LiDAR data if/when it becomes available to assess volumetric erosion/accretion.	or university. Analysis of LiDAR surveys requires considerable technical capability that generally only sits within government, engineering, Universities or research organisations.
High	Regular drone surveys to generate a time series of Digital Elevation models (DEMs). There are two approaches available a) drone-based LiDAR surveys or b) DEMs generated from drone-captured photographs. LiDAR surveys require more expensive equipment, although are becoming increasingly mainstream. LiDAR surveys could cover the entire barrier system. DEMs generated from photos would probably be cheaper, but coverage might be more limited to areas of interest (i.e. low points or areas identified as most at risk). Repeated topographic surveys of areas of concern.	Both approaches require advanced data processing capabilities. Both LiDAR and drone approaches require moderate-high performance computing. Topographic surveys have lower capability requirements but would require more time to complete and provide reduced spatial coverage. Managing the storage and analysis of the data would require moderate levels of data handling capabilities.
Mixed cost approaches	Regular low- or moderate-cost approaches could be implemented and used to trigger higher cost surveys. For example, if regular community observations revealed an erosion scarp which was potentially creating a vulnerable location on the estuary or open-coast dune, a drone survey could be commissioned.	

9. References

Albuquerque, J., Antolínez, J. A., Gorman, R. M., Méndez, F. J., & Coco, G. (2021). Seas and swells throughout New Zealand: A new partitioned hindcast. Ocean Modelling, 168, 101897.

Albuquerque, J., Antolínez, J. A., Méndez, F. J., & Coco, G. (2024). On the projected changes in New Zealand's wave climate and its main drivers. New Zealand Journal of Marine and Freshwater Research, 58(1), 89-126.

Basco, D. R., & Shin, C. S. (1999). A one-dimensional numerical model for storm-breaching of barrier islands. Journal of Coastal Research, 241-260.

Cagigal, L., Rueda, A., Castanedo, S., Cid, A., Perez, J., Stephens, S. A., ... & Méndez, F. J. (2020). Historical and future storm surge around New Zealand: From the 19th century to the end of the 21st century. International Journal of Climatology, 40(3), 1512-1525.

Cooper, J.A.G., Masselink, G., Coco, G., Short, A.D., Castelle, B., Rogers, K., Anthony, E., Green, A.N., Kelley, J.T., Pilkey, O.H. and Jackson, D.W., (2020). Sandy beaches can survive sea-level rise. Nature Climate Change, 10(11), 993-995.

Dalinghaus, C., Coco, G., & Higuera, P. (2022). A predictive equation for wave setup using genetic programming. Natural Hazards and Earth System Sciences Discussions, 2022, 1-20.

Donnelly, C., Kraus, N., & Larson, M. (2006). State of knowledge on measurement and modeling of coastal overwash. Journal of coastal research, 22(4), 965-991.

Enright, N. J., & Anderson, M. J. (1988). Recent evolution of the Mangawhai spit dunefield. Journal of the Royal Society of New Zealand, 18(4), 359-367.

Fletcher, C. H., Richmond, B. M., Barnes, G. M., & Schroeder, T. A. (1995). Marine flooding on the coast of Kaua'i during Hurricane Iniki: hindcasting inundation components and delineating washover. Journal of Coastal Research, 188-204.

Hoagland, S. W., Jeffries, C. R., Irish, J. L., Weiss, R., Mandli, K., Vitousek, S., ... & Cialone, M. A. (2023). Advances in morphodynamic modeling of coastal barriers: a review. Journal of Waterway, Port, Coastal, and Ocean Engineering, 149(5), 03123001.

Hume, T.M. 2023. Mangawhai Harbour and spit. Coastal physical processes and management. Hume Consulting Report prepared for Mangawhai Matters Inc. 22 July 2023. 77pp + app.

Kraus, N. C., Patsch, K., & Munger, S. (2008). Barrier beach breaching from the lagoon side, with reference to Northern California. Shore and Beach, 76(2), 33.

Kraus, N. C., Patsch, K., & Munger, S. (2008). Barrier beach breaching from the lagoon side, with reference to Northern California. Shore and Beach, 76(2), 33.

McCabe, P., Healy, T. R., & Nelson, C. S. (1985). Mangawhai Harbour and the development of its dual inlet system. In 1985 Australasian Conference on Coastal and Ocean Engineering (pp. 518-527). Barton, ACT: Institution of Engineers, Australia.

Ministry for the Environment. (2024). Coastal hazards and climate change guidance. Wellington: Ministry for the Environment.

Over, J. S. R., Brown, J., Sherwood, C., Hegermiller, C., Wernette, P., Ritchie, A., & Warrick, J. (2021). A survey of storm-induced seaward-transport features observed during the 2019 and 2020 hurricane seasons.

Plomaritis, T. A., Ferreira, Ó., & Costas, S. (2018). Regional assessment of storm related overwash and breaching hazards on coastal barriers. Coastal Engineering, 134, 124-133.

Sallenger Jr, A. H. (2000). Storm impact scale for barrier islands. Journal of coastal research, 890-895.

Stockdon, H. F., Holman, R. A., Howd, P. A., & Sallenger Jr, A. H. (2006). Empirical parameterization of setup, swash, and runup. Coastal engineering, 53(7), 573-588.

Stretch, D., & Parkinson, M. (2006). The breaching of sand barriers at perched, temporary open/closed estuaries—a model study. Coastal Engineering Journal, 48(01), 13-30.

Tonkin & Taylor (2021). Coastal Flood Hazard Assessment for Northland Region 2019-2020. Prepared for Northland Regional Council.

Vos, K., Harley, M. D., Splinter, K. D., Simmons, J. A., & Turner, I. L. (2019). Sub-annual to multi-decadal shoreline variability from publicly available satellite imagery. Coastal Engineering, 150, 160-174.

Figure 1. Digital Elevation Model from 2018 LiDAR survey

Figure 2. Hillshade model from 2018 LiDAR survey

Figure 3. Digital Elevation Model from 2024 Drone LiDAR survey

Figure 4. Hillshade model from 2024 Drone LiDAR survey

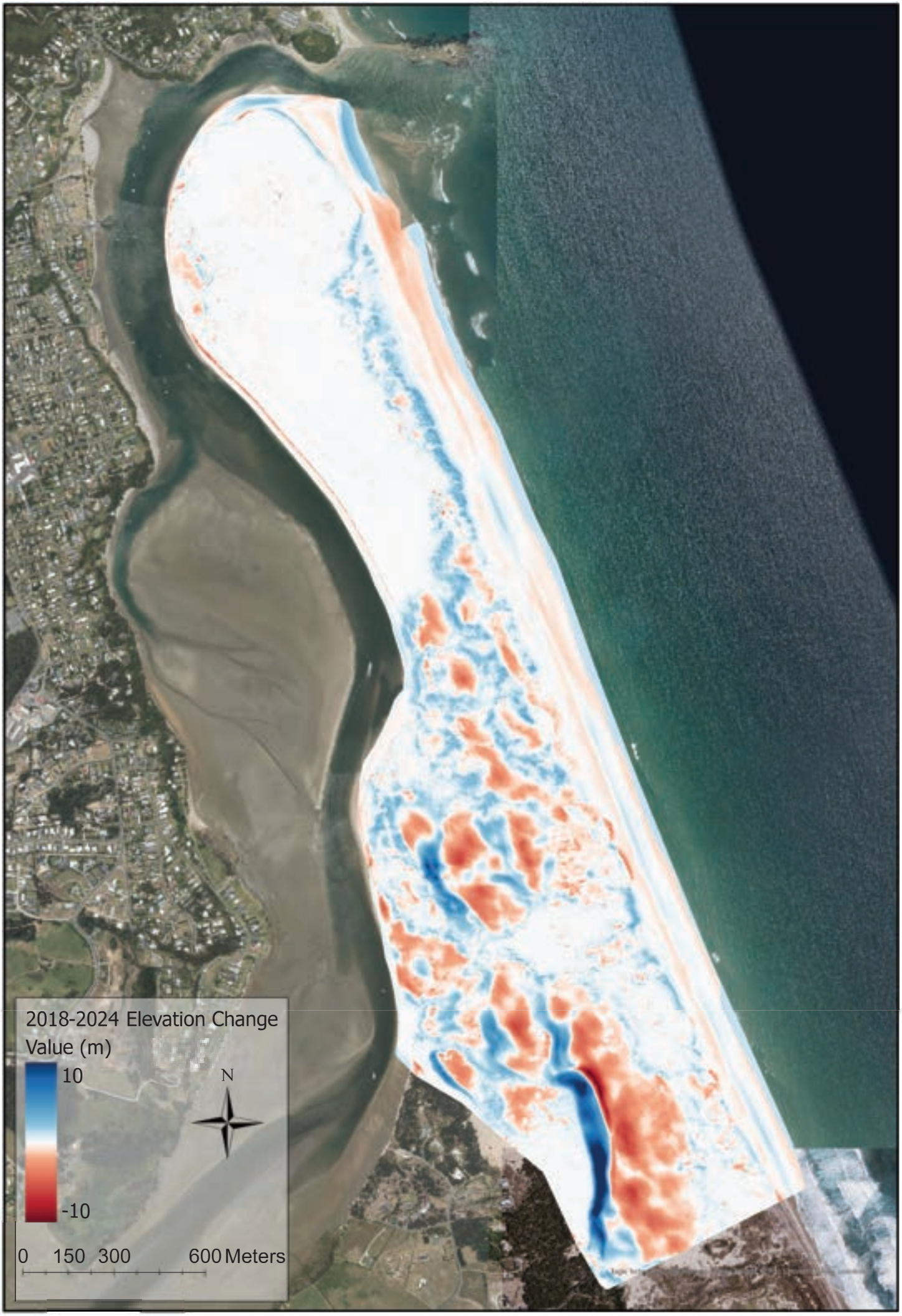

Figure 5. DEM-of-difference (2018 v 2024)

Figure 6. Cut-and-fill analysis to evaluate the net gain and loss of sand (2018 v 2024)

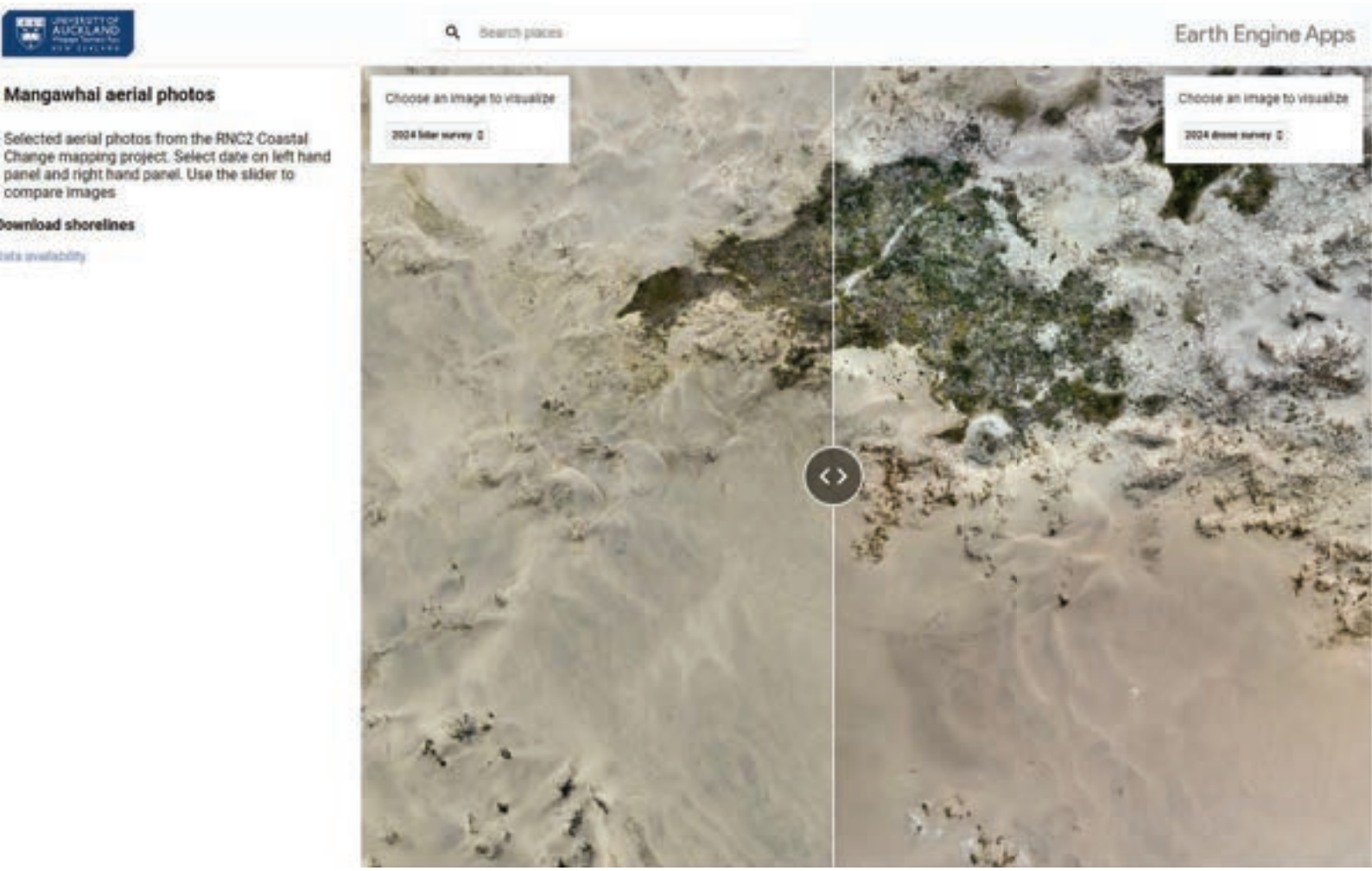

Figure 7. Web map showing visual comparison of 2024 LiDAR mosaic and SfM mosaic
https://murrayford.users.earthengine.app/view/mangawhai-aerial-viewer

Figure 8. Slope map and water flow direction

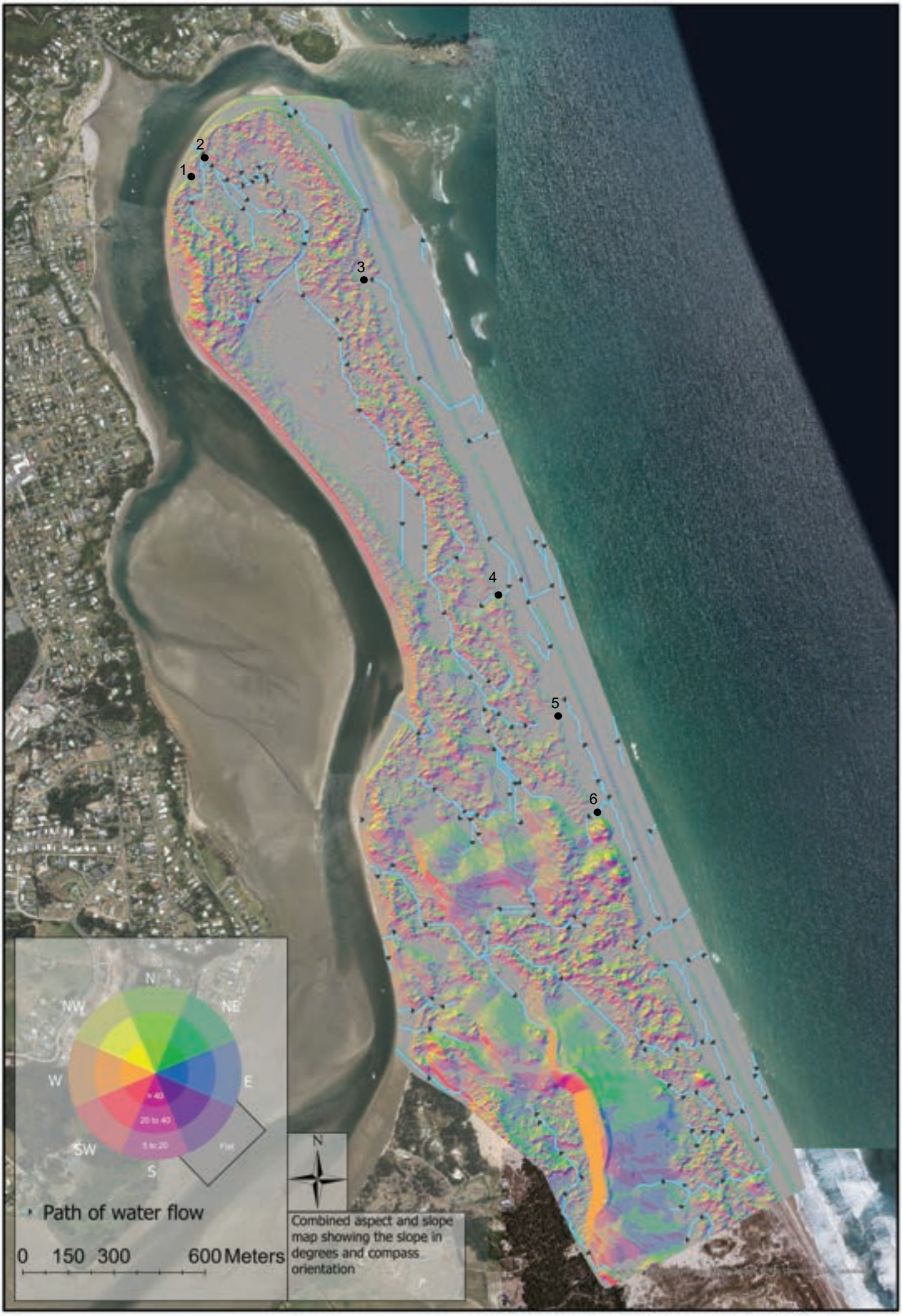

Figure 9. Slope map and aspect and numbered potential vulnerable inundation points

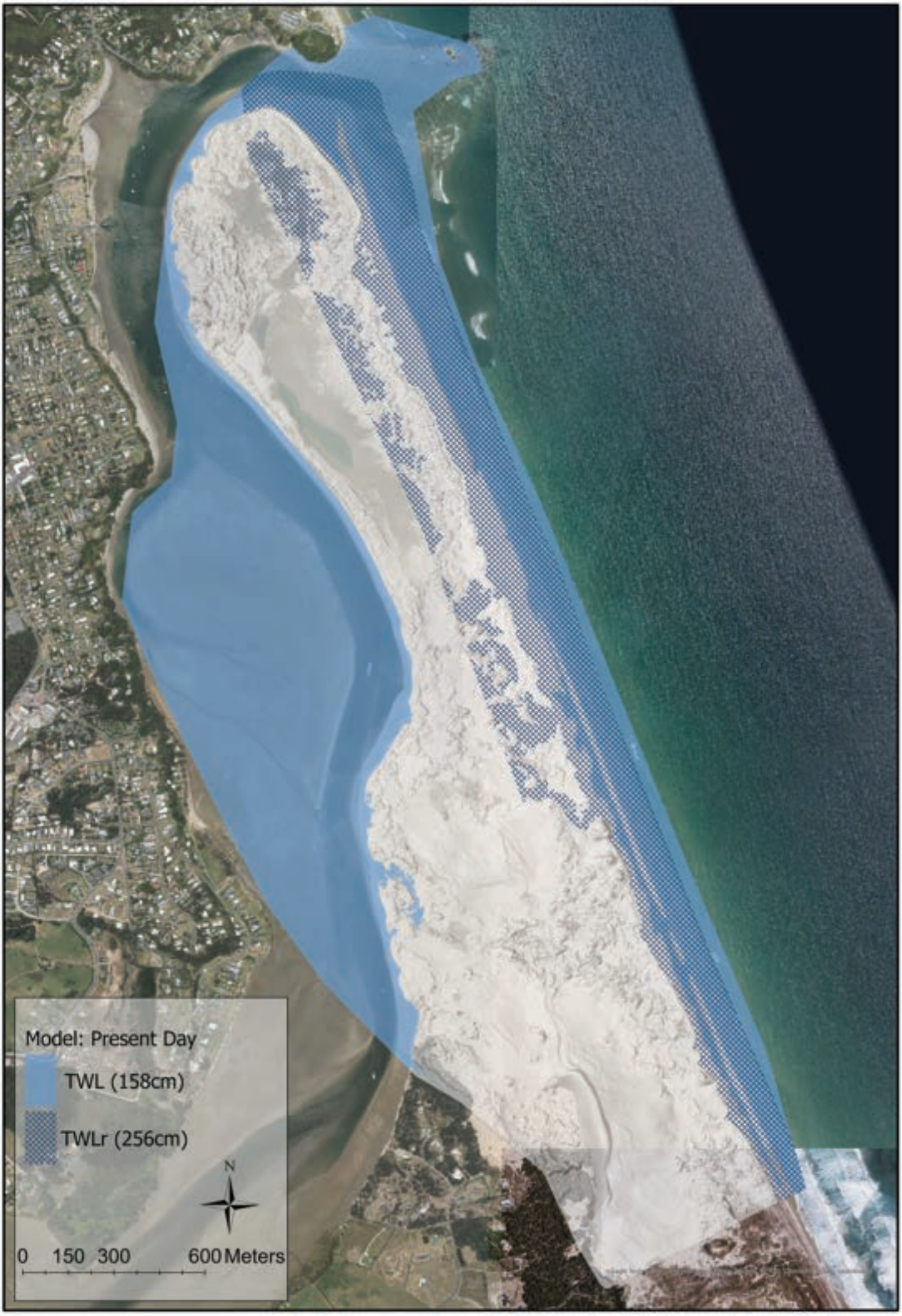

Figure 10. Bathtub inundation for 2024 (present day) showing TWL and TWLr

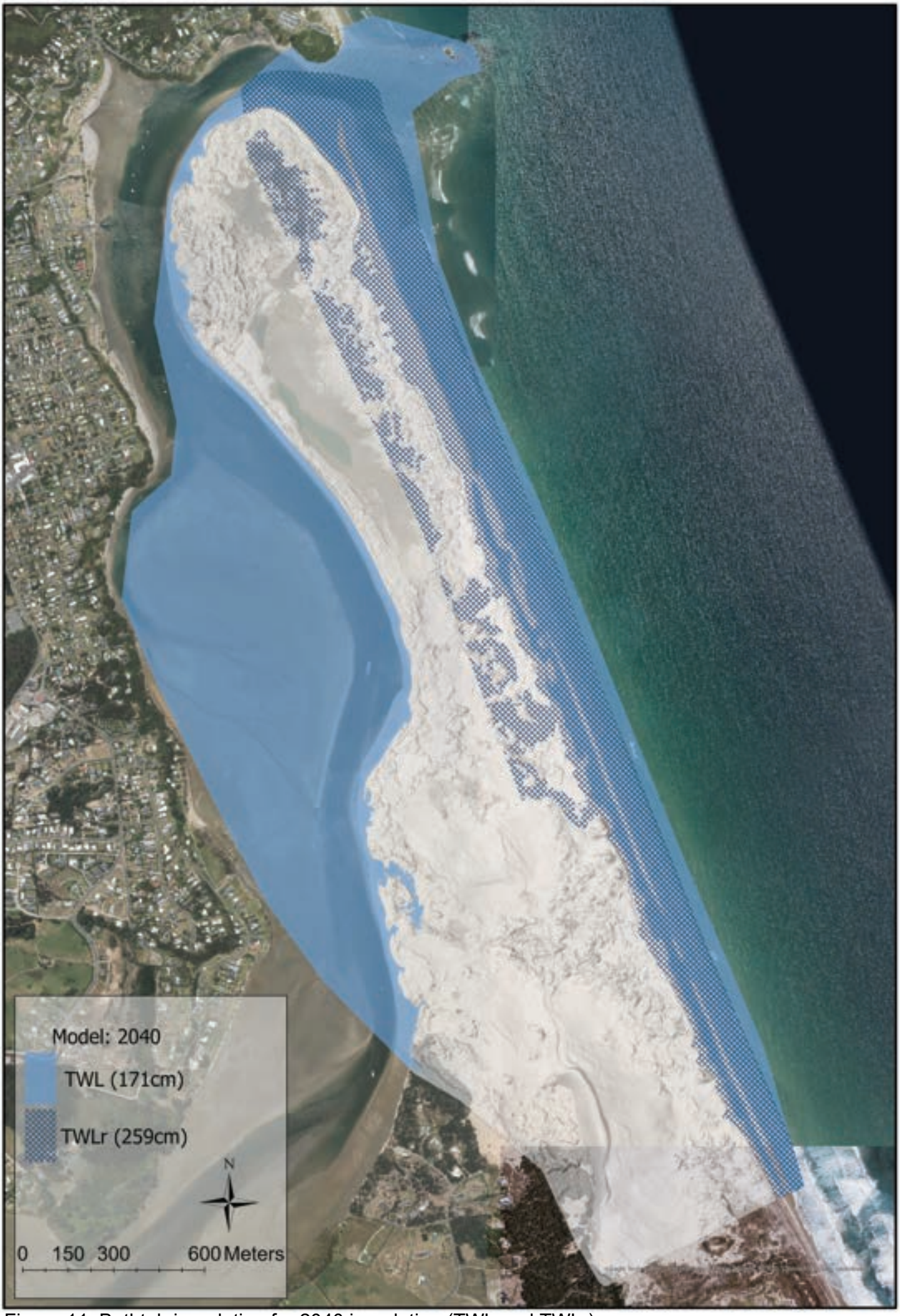

Figure 11. Bathtub inundation for 2040 inundation (TWL and TWLr)

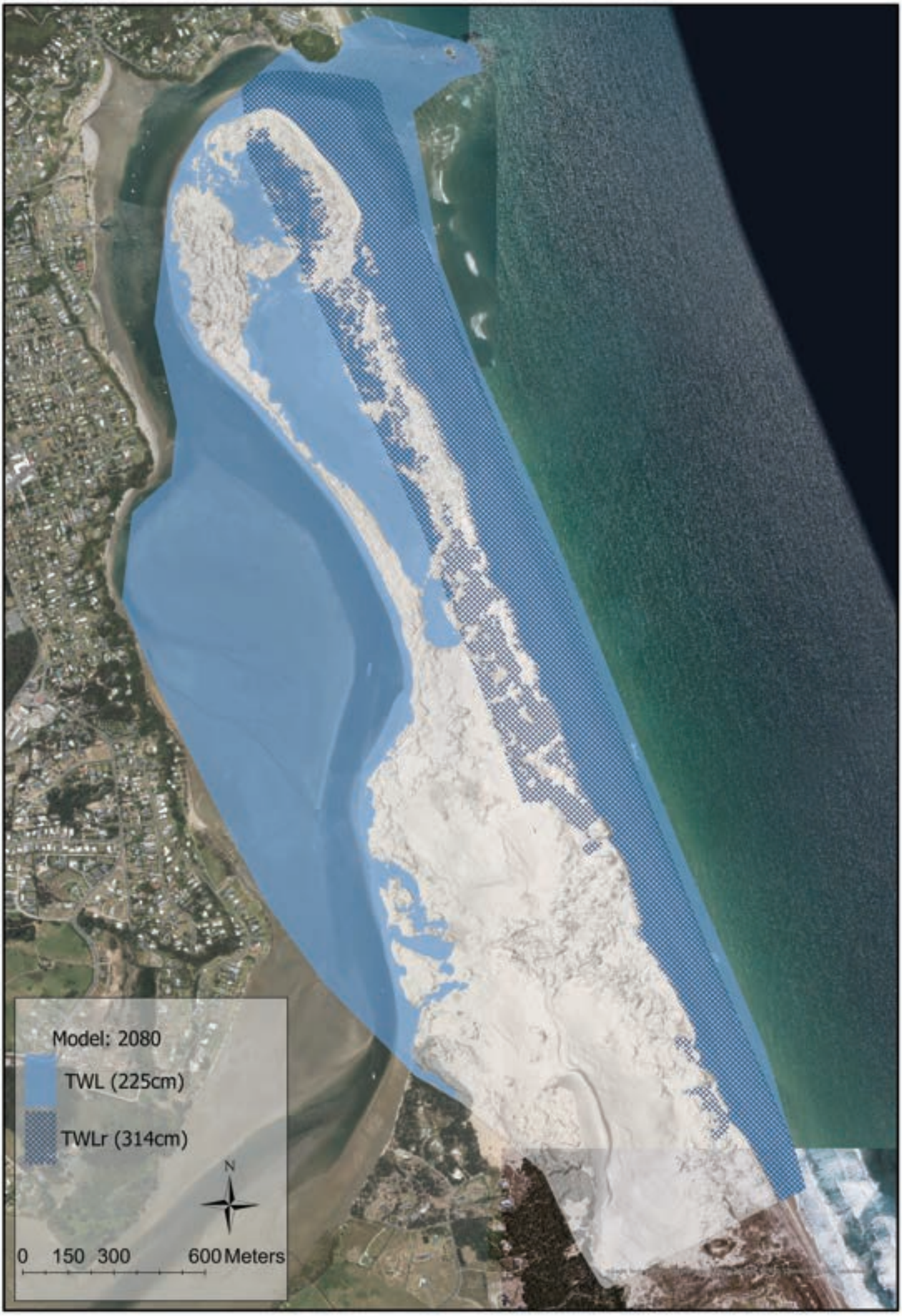

Figure 12. Bathtub inundation for 2080 inundation (TWL and TWLr)

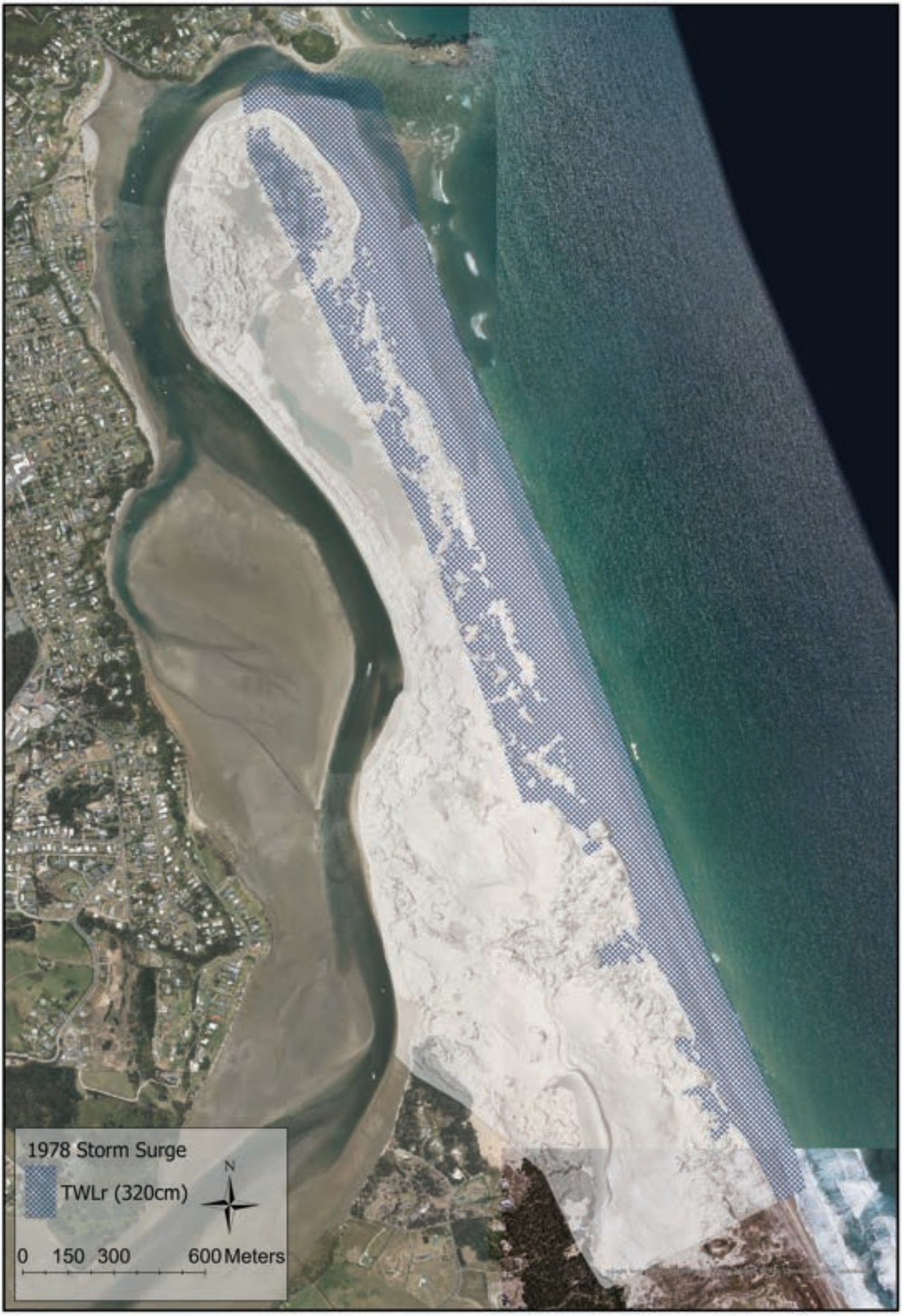

Figure 13. Bathtub inundation for comparable storm to 1978 (TWLr)

Figure 14. Bathtub inundation for 1% ARI storm (dynamic TWLr) present day

Figure 15. Web map showing historic aerial photographs for Mangawhai
https://murrayford.users.earthengine.app/view/mangawhai-aerial-viewer

Figure 16. Web map showing historic coastlines for Mangawhai
https://murrayford.users.earthengine.app/view/mangawhaiaerialsandlines

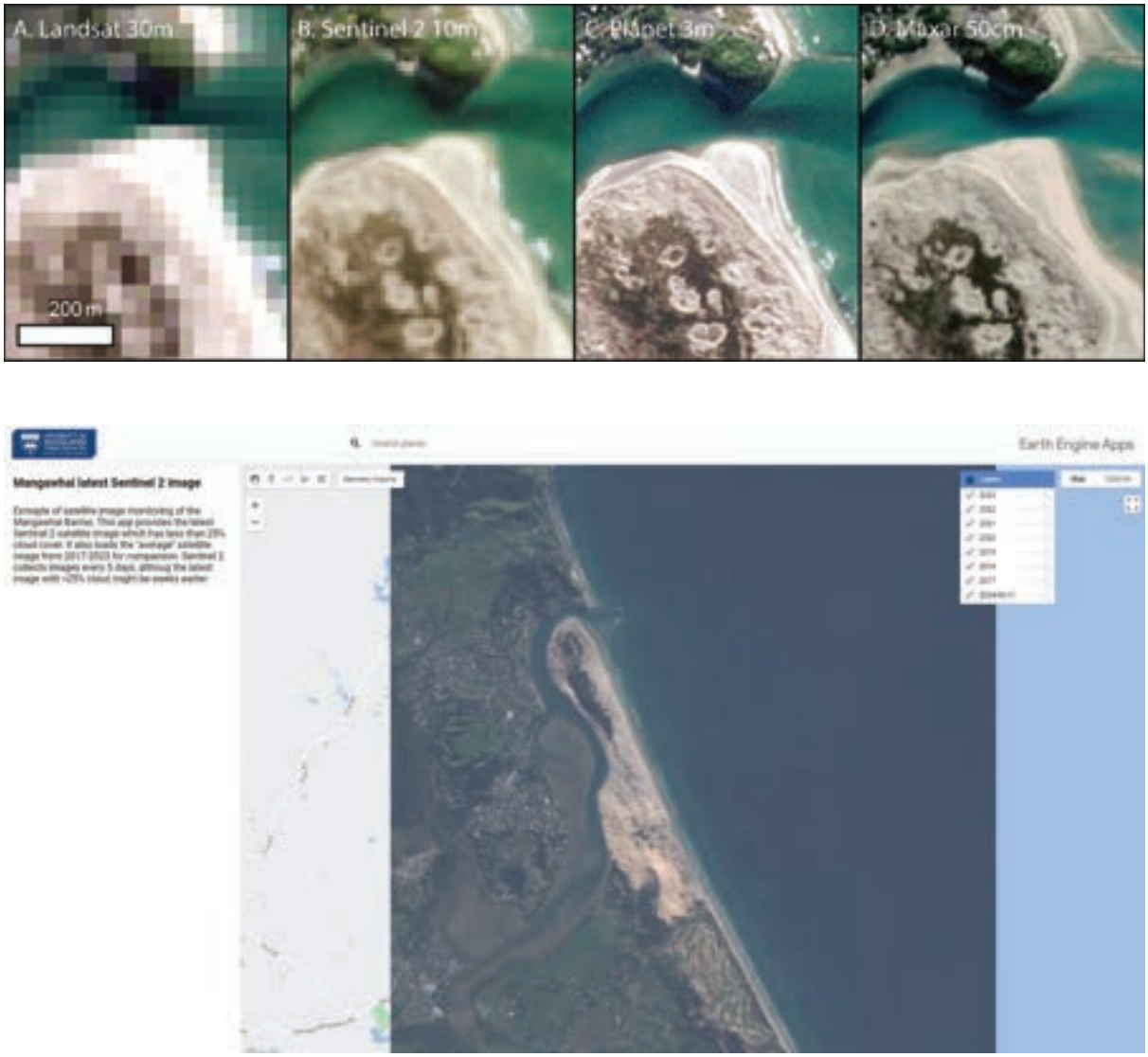

Figure 17. Web map showing example freely available satellite images
https://murrayford.users.earthengine.app/view/mangawhais2viewer